Nanocrystalline TiO$_2$ Solar Cells Sensitized with InAs Quantum Dots[†]

Pingrong Yu,*,‡ Kai Zhu, Andrew G. Norman, Suzanne Ferrere, Arthur J. Frank, and Arthur J. Nozik*

Center for Basic Sciences, National Renewable Energy Laboratory, Golden, Colorado 80401

Received: July 27, 2006; In Final Form: September 29, 2006

We report nanocrystalline TiO$_2$ solar cells sensitized with InAs quantum dots. InAs quantum dots of different sizes were synthesized and incorporated in solar cell devices. Efficient charge transfer from InAs quantum dots to TiO$_2$ particles was achieved without deliberate modification of the quantum dot capping layer. A power conversion efficiency of about 1.7% under 5 mW/cm^2 was achieved; this is relatively high for a nanocrystalline metal oxide solar cell sensitized with presynthesized quantum dots, but this efficiency could only be achieved at low light intensity. At one sun, the efficiency decreased to 0.3%. The devices are stable for at least weeks under room light in air.

Introduction

Semiconductor quantum dots (QDs) have several properties that are potentially attractive for applications in solar cells. Since the QD band gap (HOMO−LUMO energy) can be tuned by simply changing the QD size,[1−4] their optical properties can be tailored to maximize solar photon absorption. Furthermore, QDs have been shown recently to produce highly efficient multiple exciton generation (MEG), whereby a single absorbed photon can generate more than one electron−hole pair;[5−7] in QDs, electron−hole pairs are highly correlated and form excitons. Ultrafast transient absorption spectroscopy has shown that in colloidal solutions of PbSe quantum dots, three excitons/photon can be generated upon absorbing photons with energies 4 times the QD band gap[5,6] and seven excitons/photon can be generated with photons 8 times the QD band gap.[8] A thermodynamic analysis[9] of the maximum theoretical power conversion efficiencies for solar cells on the basis of MEG shows that with two excitons/photon the ultimate efficiency at one sun is ∼42%, with three excitons/photon it is ∼43%, and with N excitons produced by photons with energies N times the band gap the efficiency reaches ∼44% for $N \gg 3$. For photovoltaic cells that produce just one exciton/photon, the maximum theoretical efficiency at one sun is ∼32%.[10] Thus, the conversion efficiency saturates rapidly with increasing values of excitons generated per photon, and most (94%) of the additional gain in efficiency from MEG is obtained with only two excitons/photon. For MEG solar cells, the optimum QD band gap shifts moderately to the red, and the maximum efficiency upon the generation of two excitons/photon occurs at a QD band gap of ∼1 eV;[9] for conventional solar cells, the optimum band gap ranges from 1.2 to 1.4 eV.

There are several configurations for solar cells that use QDs to take advantage of MEG.[11] The one we focus on here is to replace the dye molecules that are adsorbed onto the nanocrystalline TiO$_2$ film in a dye-sensitized solar cell (so-called Grätzel cell)[12] with QDs to make a QD-sensitized solar cell

(QDSSC).[13−16] As stated above, for high-efficiency solar conversion, the band gap of the QD needs to be about 1 eV. Thus, because size quantization increases the band gap of bulk semiconductors, and small effective masses are generally associated with small band gap semiconductors which then cause very pronounced band gap increases with decreasing QD size, the required bulk band gap for semiconductors used as QDs in QDSSCs needs to be in the range of ∼0.3−0.5 eV. InAs has an appropriate bulk band gap of 0.36 eV and is also rather stable in the liquid electrolytes required for sensitized nanocrystalline TiO$_2$ solar cells. Although MEG has not yet been demonstrated in InAs QDs, we first study their general behavior as sensitizers in a QDSSC.

Several groups have demonstrated that QDSSCs work (not considering MEG effects), but the efficiencies are very low and there are significant stability issues. Gopidas et al., Hotchandani and Kamat,[17,18] and Spanhel et al.[19] described photoinduced charge transfer between CdS QDs and TiO$_2$ nanoparticles. Later, Vogel et al. did a comparison of a variety of QD sulfides as sensitizers matched to different nanocrystalline oxides in a sensitized solar cell (SSC) configuration,[13] and Fang et al. reported the sensitization of TiO$_2$ with CdSe.[14] Recently, Plass et al. described a PbS QD sensitized nanocrystalline TiO$_2$ solar cell in which spiro-OMeTAD was used as a hole conductor.[16] Zaban et al. reported the sensitization of TiO$_2$ with the III−V semiconductor InP that had been first synthesized, fully characterized, and then adsorbed to the TiO$_2$ surface.[15] In contrast, the metal chalcogenides are typically grown directly in situ in the pores of the TiO$_2$ nanocrystalline film. Presynthesis and purification followed by adsorption allow greater control over the size, shape, and surface properties of the QDs.

Here, we present results for InAs QDs as sensitizers in the QDSSC.[20] The InAs QDSSC devices are very stable, reproducible, and exhibit a relatively high efficiency (compared to other QD sensitizers), even in the absence of sophisticated linkage chemistry to the TiO$_2$ nanoparticles. The power conversion efficiency was estimated to be ∼1.7% under low simulated solar illumination intensity (5 mW/cm^2); under higher (one sun) light intensities of 100 mW/cm^2 the efficiency dropped to 0.3%. To our knowledge, the 1.7% conversion efficiency at 5 mW/cm^2 is the highest reported value (at equivalent low light intensity)

for QDSSCs sensitized with presynthesized QDs. With CdSe nanostructures grown in situ on the surface of TiO$_2$, Niitsoo et al were able to achieve 2.8% conversion efficiency[21] at full solar intensity. However, in this case, the nature of the CdSe nanostructures were not fully characterized. Future refinement and optimization of the InAs/TiO$_2$ QDSSC system, together with possible MEG effects, should lead to much improved photovoltaic performance.

Experimental Section

Unless otherwise noted, all chemicals were obtained from Aldrich and were used without further purification. All steps are carried out in a strictly air/water-free environment, either in the glovebox or on a Schlenk vacuum line.

Tris(trimethylsilyl)arsine (As[TMS]$_3$) was synthesized by reaction of reduced As with Me$_3$SiCl.[22] Na/K alloy was prepared from 9.6 g Na and 13.7 g K and was filtered through a coarse glass filter. The alloy was slowly added through a glass stopcock over a period of 2 h to a 1-L three-neck flask containing 16.5 g As powder and 350 mL dry dimethoxyethane (DME), under stirring with a stainless steel stir bar. The dark mixture was heated at reflux overnight. After that, 105 mL of Me$_3$SiCl was added dropwise to the cooled mixture and the orange-brown suspension was again refluxed overnight. The suspension was then filtered with cannula filter sticks and was washed with 200 mL DME. DME was removed from the combined filtrates under reduced pressure, and the residue was vacuum distilled (bp 48 °C at 10^{-3} Torr) to obtain As[TMS]$_3$.

InAs nanocrystalline QDs were prepared from InCl$_3$ and As-[TMS]$_3$ as reported previously.[23,24] A room-temperature precursor mixture of typically 0.76 M As[TMS]$_3$, 1.1 M InCl$_3$, and 0.20% trioctylphosphine oxide (TOPO) in trioctylphosphine (TOP) was prepared. The precursor mixture was then injected into 300 °C TOP under an inert atmosphere to grow QDs. The QD size was controlled by growth time and the number of subsequent injections after the initial nucleation; size-selective precipitation in toluene/methanol solutions was performed to obtain narrower size distributions.

Nanocrystalline TiO$_2$ films were prepared and assembled into SSCs as previously reported.[25−28] Films with typical areas of 0.1−0.2 cm^2 and 4−16 μm thickness were dipped into solutions of InAs QDs in toluene in the glovebox till the films became dark. The devices were assembled in a sandwich configuration with the TiO$_2$ film facing a counter electrode, prepared by spreading a droplet of 5 mM H$_2$PtCl$_6$ in 2-propanol onto TEC8 conducting glass plates and subsequently firing them at 350 °C for 30 min.[25] All solar cells were assembled as described elsewhere.[26] The electrolyte solution was 0.2 M [Co^{II}(4,4′-di-*tert*-butyl-2,2′-bipyridyl)$_3$]{ClO$_4$}$_2$ and 0.1 M lithium triflate in methoxyproprionitrile, developed by Nusbaumer et al.[29] The 0.02 M nitrosonium tetrafluoroborate (NOBF$_4$) was added to the solution which oxidizes Co^{II} to Co^{III}, and the solution was degassed with nitrogen to expel nitric oxide (NO). Electrolyte based on iodide/triiodide redox couple[30] was also tested.

Current−voltage (*J*−*V*) measurements were performed using a home-built solar simulator based on a metal halide lamp with output intensity adjusted to AM1.5 100 mW/cm^2.[25] A calibrated Si photodetector fitted with a KG-5 filter (Schott) was used as a reference. The spectra mismatch error[31] of this setup is less than 5% for InAs QDs sensitized solar cells. Calibrated neutral density optical filters were used to vary the incident light intensity. The incident photon-to-current conversion efficiency (IPCE) measurements were performed with a Photon Technology International Model 1492 monochromator.[25] The mono-
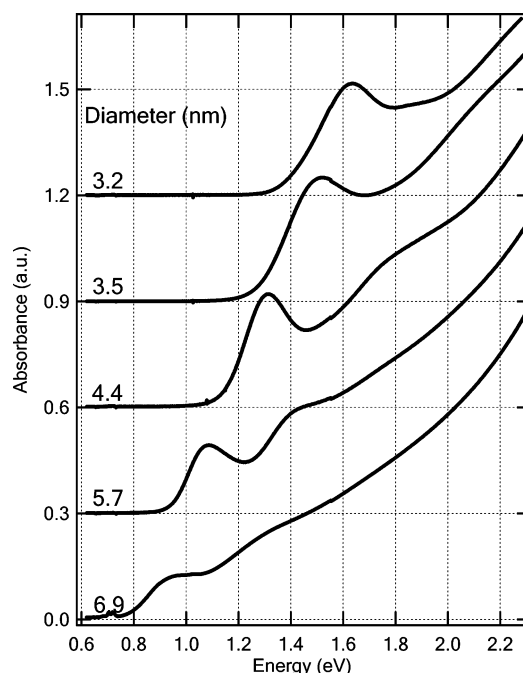

Figure 1. Absorption spectra of InAs QDs of different sizes. Plots are vertically displaced for clarity.
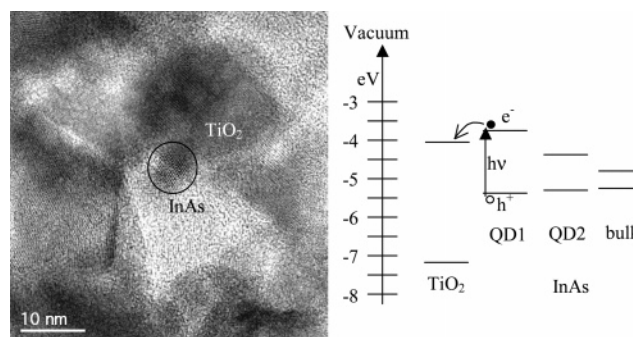

Figure 2. Left: InAs/TiO$_2$ high-resolution TEM image. The image of a ∼6 nm InAs QD is circled. The TiO$_2$ particles are about 20 nm in diameter. Right: energetics of TiO$_2$ and InAs QDs and bulk.

chromatic light was modulated with an optical chopper (Stanford Research Systems model 540), and the light intensity was measured with a calibrated Si photodiode connected to a lock-in amplifier (SRS model 830). A second lock-in amplifier was used to measure the photocurrent response from the sample.

All absorption spectra are taken with a Cary 500 double beam spectrometer.

Results and Discussions

Figure 1 shows the relationship between the absorbance spectra of InAs QDs with their sizes indicated by their average diameters. As the QD diameter decreases from 6.9 to 3.2 nm, the first exciton absorption peak blue shifts from 0.9 to 1.65 eV because of quantum confinement effects.[1,2]

Figure 2 shows a typical high-resolution TEM image of InAs QDs and TiO$_2$ nanoparticles used in our QDSSCs. Intimate contact between the InAs QDs and TiO$_2$ particles was observed. Upon absorbing an incident photon, an electron−hole pair (exciton) is generated within a QD. To have an energetic driving force for efficient charge separation/injection, the excited states of the QDs must be higher than the conduction bandedge of TiO$_2$. The III−V semiconductor InAs makes for interesting flexibility in this regard. Its bulk band gap is 0.36 eV, and the

Nanocrystalline TiO$_2$ Solar Cells

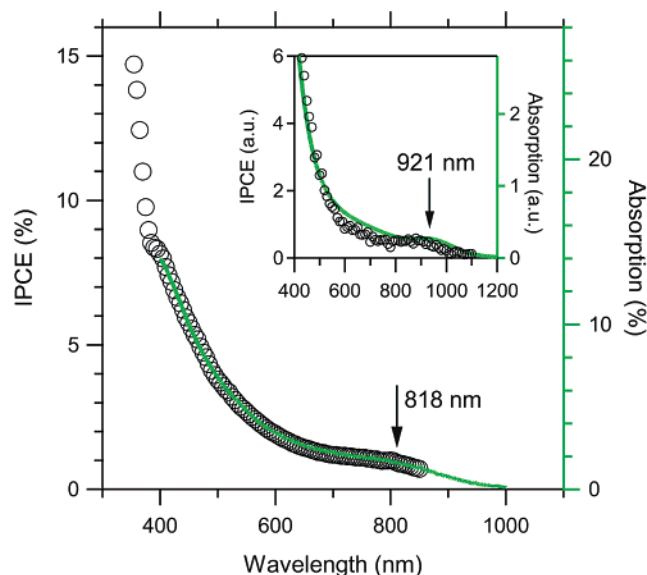*J. Phys. Chem. B, Vol. 110, No. 50, 2006* **25453**

Figure 3. Open circles: IPCE of a QDSSC using 3.4-nm InAs QD sensitizers. Green line: absorption spectrum of the 3.4-nm InAs QDs. The IPCE and absorption spectra essentially overlap and both show the 818-nm first exciton absorption peak of the 3.4-nm InAs QDs, indicated with an arrow. Inset: IPCE of a QDSSC using 4.5-nm InAs QDs and the QD absorption spectrum, with both showing the first exciton absorption peak of the 4.5-nm InAs QDs at 921 nm.

Figure 4. $J-V$ characteristic of a QDSSC with 3.4-nm InAs QD sensitizers under different illumination intensities. The conversion efficiencies, 1.74% and 0.3%, are labeled for the 5 and 100 mW/cm^2 illumination, respectively.

colloidal QDs, because of quantization, typically have an absorption range that spans the visible to near-infrared region, as shown in Figure 1. The effective mass of the electron (0.023 m$_0$) is much smaller than that of the hole (0.41 m$_0$); thus, the increase in band gap will have a proportionately larger effect on the conduction band than on the valence band, that is, as the QDs become smaller, the conduction band will shift to a much greater extent than the valence band. This feature facilitates systematical studies of the driving force dependence on the charge injection process in QDSSCs. Similar studies in a molecular system would typically require structural, chemical, and functional changes at the same time; thus, a well-controlled system in which only one variable changes is very difficult with dye molecules. On the basis of the band positions of TiO$_2$[32] and InAs[33] and of the effective masses of electrons and holes of InAs,[33] it was estimated that the band gap of an InAs QD has to be larger than 1.2 eV to inject electrons into TiO$_2$. Figure 2 shows a schematic diagram of energy levels of TiO$_2$ nanoparticles and InAs QDs as a function of arbitrary size.

To complete the electrical circuit in a solar cell, the valence band of the InAs QDs needs to be lower (more positive) than the redox potential of the redox couple relay system in the electrolyte. The valence band of bulk InAs (-5.3 eV vs Vacuum[33]) is significantly lower than the redox potentials of Co^{2+}/Co^{3+} (-4.89 eV vs Vacuum[29]) and I$^-$/I$_3^-$ (-4.94 eV vs Vacuum[32]) used in this study. Since the valence band of InAs QDs is lower than that of InAs bulk, the regeneration of InAs QDs by the redox couple in the electrolyte is therefore energetically favored.

Figure 3 shows a typical IPCE spectrum and optical absorption spectrum of InAs QDs. The latter is obtained by subtracting the blank (no QDs) device absorption from a working device absorption. The average QD size is 3.4 nm in diameter with the first exciton absorption peak at 818 nm. IPCE was measured under monochromatic illumination modulated with a chopper at 8 Hz. Although IPCE is likely underestimated because of the mechanical limitation of optical chopping, the good match of spectral shapes between the IPCE and absorption measure-
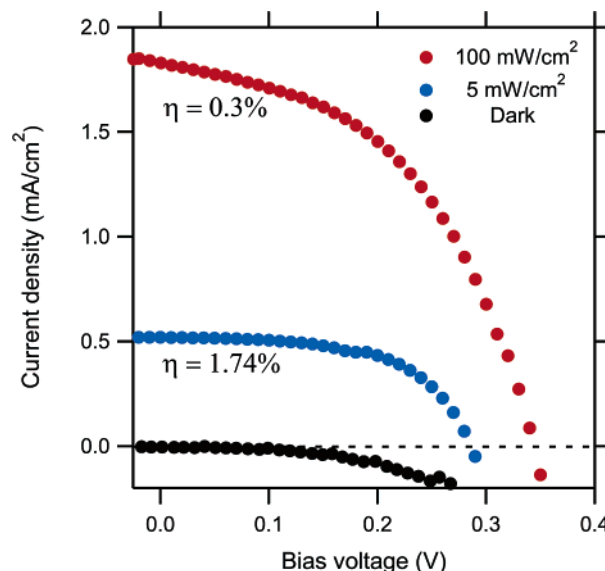
ments indicates that the photocurrent results from the photo-excitation of InAs QDs. A clear shoulder (indicated by arrow) appears in both the IPCE and absorption spectra; this position corresponds to the band gap of 3.4-nm InAs QDs. The inset shows the IPCE and absorption spectra for a typical cell with an average of 4.5-nm QD sensitizers whose first exciton absorption is at 921 nm; both IPCE and absorption spectra follow essentially the same trend as those of the 818-nm sample. Measurements of QDSSCs with InAs QDs having the first exciton absorption at 1055 nm (1.18 eV) and 1365 nm (0.91 eV) showed no measurable IPCE and very low cell efficiency. This concurs with the calculation of 1.2 eV as being the minimum band gap required for charge injection.

Figure 4 shows the $J-V$ characters of one of our most efficient QDSSCs sensitized with InAs QDs. The average QD size is 3.4 nm in diameter with the first exciton absorption peak at 818 nm. The measurements under simulated AM1.5 sunlight illumination at 5 mW/cm^2 showing a power conversion efficiency of ~1.7% exhibited a fill factor of 0.58. A reference sample without InAs QDs indicated that the photocurrent density generated from just the TiO$_2$ and Co redox relay was negligible compared to that of samples sensitized with InAs QDs. The relatively high conversion efficiency indicates that InAs QDs are efficient sensitizers for TiO$_2$-based nanocrystalline solar cells. Optimization of the particle surface,[25,34-36] film thickness,[37] amount of QDs adsorbed onto TiO$_2$, good molecular charge-conducting linkers between the QDs and TiO$_2$ particles,[38] electrolyte recipe,[29] and TiO$_2$ particle size[30] are expected to further increase the efficiency.

The drop in solar power conversion efficiency from 1.7% at 5 mW/cm^2 to 0.3% at 100 mW/cm^2, shown in Figure 4, is due primarily to the fact that the photocurrent density only increases by a factor of 3.5 as the incident light intensity increases by a factor of 20. Although under 100 mW/cm^2 illumination, the open-circuit voltage (V_{oc}) increased to 0.35 V from 0.29 V under 5 mW/cm^2, fill factor decreased from 0.58 to 0.48. In a recent study on dye-sensitized solar cells using the same cobalt compounds as redox couple relays, the power conversion efficiencies were found to decrease by a factor of 2 when the incident AM1.5 light intensity increased from 10 to 100 mW/cm^2; the drop in efficiency was attributed to the limitation of

mass transport of the redox relay at higher light intensity.[29] A similar efficiency drop with increasing light intensity was also observed in another recent paper on CdSe QD sensitized TiO$_2$ nanocrystalline solar cells using aqueous Na$_2$S solution as electrolye.[38] At approximately 100 mW/cm^2 of the incident light, these authors found that the photocurrent density decreased immediately upon illumination and stabilized at about 45% of the initial photocurrent value on the time scale of seconds; the photocurrent decay was attributed to the enhanced back recombination of electrons in TiO$_2$ with holes in QDs at higher incident light intensity.[38] We believe that these two effects also likely caused lower conversion efficiency at higher light intensity in our system.

Finally, we note that the sealed QDSSCs are chemically stable for weeks in air under room light without a significant drop in their power conversion efficiency. On the other hand, cells using iodide-based electrolyte corrode within minutes, and no reliable photovoltaic characterizations can be performed using this redox relay system.

Conclusions

Relatively efficient and stable InAs QD sensitized TiO$_2$ solar cells are demonstrated, with the highest power conversion efficiency of ∼1.7% achieved under simulated solar illumination AM1.5 5 mW/cm^2 using 3.4-nm InAs QDs and a Co redox system as the charge-transfer relay. Only InAs QDs with a band gap greater than 1.2 eV show a photovoltaic effect, which is consistent with our band alignment estimates. The solar cells show lower power efficiency under higher light intensity, probably because of both mass transport limitations of the redox relay and also the increased charge recombination from the back reaction of electrons in TiO$_2$ with holes in QDs. Better solar cell performance may be expected with further modification and optimization.

References and Notes

(1) Efros, A. L.; Efros, A. L. *Sov. Phys. -Semiconductors* **1982**, *16*, 772.
(2) Brus, L. *J. Phys. Chem.* **1986**, *90*, 2555.
(3) Alivisatos, A. P. *J. Phys. Chem.* **1996**, *100*, 13226.
(4) Micic, O. I.; Cheong, H. M.; Fu, H.; Zunger, A.; Sprague, J. R.; Mascarenhas, A.; Nozik, A. J. *J. Phys. Chem.* **1997**, *101*, 4904.
(5) Schaller, R. D.; Klimov, V. I. *Phys. Rev. Lett.* **2004**, *92*, 186601.
(6) Ellingson, R. J.; Beard, M.; Johnson, J. C.; Yu, P.; Micic, O. I.; Nozik, A. J.; Shabaev, A.; Efros, A. L. *Nano Lett.* **2005**, *5*, 865.
(7) Murphy, J. E.; Beard, M.; Norman, A. G.; Ahrenkiel, S. P.; Johnson, J. C.; Yu, P.; Micic, O. I.; Ellingson, R. J.; Nozik, A. J. *J. Am. Chem. Soc.* **2006**, *128*, 3241.
(8) Schaller, R. D.; Sykora, M.; Pietryga, J. M.; Klimov, V. I. *Nano Lett.* **2006**, *6*, 424.
(9) Hanna, M.; Nozik, A. J. *J. Appl. Phys.* in press.
(10) Shockley, W.; Queisser, H. J. *J. Appl. Phys.* **1962**, *32*, 510.
(11) Nozik, A. J. *Physica E* **2002**, *14*, 115.
(12) O'Regan, B.; Grätzel, M. *Nature (London)* **1991**, *353*, 737.
(13) Vogel, R.; Hoyer, P.; Weller, H. *J. Phys. Chem.* **1994**, *98*, 3183.
(14) Fang, J.; Wu, J.; Lu, X.; Shen, Y.; Lu, Z. *Chem. Phys. Lett.* **1997**, *270*, 145.
(15) Zaban, A.; Micic, O. I.; Gregg, B. A.; Nozik, A. J. *Langmuir* **1998**, *14*, 3153.
(16) Plass, R.; Pelet, S.; Krueger, J.; Grätzel, M.; Bach, U. *J. Phys. Chem. B* **2002**, *106*, 7578.
(17) Gopidas, K. R.; Bohorquez, M.; Kamat, P. V. *J. Phys. Chem.* **1990**, *94*, 6435.
(18) Hotchandani, S.; Kamat, P. V. *J. Phys. Chem.* **1992**, *96*, 4.
(19) Spanhel, L.; Weller, H.; Henglein, A. *J. Am. Chem. Soc.* **1987**, *109*, 6632.
(20) Yu, P. Ph.D. Thesis, University of Colorado at Boulder, 2004.
(21) Niitsoo, O.; Sarkar, S. K.; Pejoux, C.; Ruhle, S.; Cahen, D.; Hodes, G. *J. Photochem. Photobiol., A-Chem.* **2006**, *181*, 306.
(22) Becker. *Z. Anorg. Allg. Chem.* **1980**, *462*, 113.
(23) Yu, P.; Beard, M.; Ferrere, S.; Ellingson, R. J.; Curtis, C.; Drexler, J.; Luiszer, F.; Nozik, A. J. *J. Phys. Chem. B* **2005**, *109*, 7084.
(24) Cao, Y.; Banin, U. *J. Am. Chem. Soc.* **2000**, *122*, 9692.
(25) Neale, N. R.; Kopidakis, N.; van de Lagemaat, J.; Grätzel, M.; Frank, A. J. *J. Phys. Chem. B* **2005**, *109*, 23183.
(26) Benkstein, K. D.; Kopidakis, N.; van de Lagemaat, J.; Frank, A. J. *J. Phys. Chem. B* **2003**, *107*, 7759.
(27) Ferrere, S. *Chem. Mater.* **2000**, *12*, 1083.
(28) Zaban, A.; Ferrere, S.; Sprague, J.; Gregg, B. A. *J. Phys. Chem. B* **1997**, *101*, 55.
(29) Nusbaumer, H.; Zakeeruddin, S. M.; Moser, J.; Grätzel, M. *Chem.—Eur. J.* **2003**, *9*, 3756.
(30) Kopidakis, N.; Neale, N. R.; Zhu, K.; van de Lagemaat, J.; Frank, A. J. *Appl. Phys. Lett.* **2005**, *87*.
(31) Emery, K. A.; Osterwald, C. R.; Aharoni, H. *Solid-State Electron.* **1987**, *30*, 213.
(32) Hagfeldt, A.; Grätzel, M. *Chem. Rev.* **1995**, *95*, 49.
(33) http://www.ioffe.rssi.ru/SVA/NSM/Semicond/InAs/.
(34) Park, N. G.; Schlichthörl, G.; van de Lagemaat, J.; Cheong, H. M.; Mascarenhas, A.; Frank, A. J. *J. Phys. Chem. B* **1999**, *103*, 3308.
(35) Ito, S.; Liska, P.; Comte, P.; Charvet, R. L.; Pechy, P.; Bach, U.; Schmidt-Mende, L.; Zakeeruddin, S. M.; Kay, A.; Nazeeruddin, M. K.; Gratzel, M. *Chem. Commun.* **2005**, 4351.
(36) Palomares, E.; Clifford, J. N.; Haque, S. A.; Lutz, T.; Durrant, J. R. *J. Am. Chem. Soc.* **2003**, *125*, 475.
(37) Fisher, A. C.; Peter, L. M.; Ponomarev, E. A.; Walker, A. B.; Wijayantha, K. G. U. *J. Phys. Chem. B* **2000**, *104*, 949.
(38) Robel, I.; Subramanian, V.; Kuno, M.; Kamat, P. V. *J. Am. Chem. Soc.* **2006**, *128*, 2385.